Effect of large-scale kinetic power extraction on time-dependent estuaries

B Polagye[1*], **P Malte**[1], **M Kawase**[2], and **D Durran**[3]

[1]Department of Mechanical Engineering, University of Washington, Seattle, Washington, USA

[2]School of Oceanography, University of Washington, Seattle, Washington, USA

[3]Department of Atmospheric Sciences, University of Washington, Seattle, Washington, USA

The manuscript was received on 28 August 2007 and was accepted after revision for publication on 14 April 2008.

DOI: 10.1243/09576509JPE519

Abstract: An open and important question in tidal in-stream energy conversion is the level of kinetic power extraction that is possible without unacceptable environmental degradation. In general, the effects of large-scale kinetic power extraction on estuary-scale fluid mechanics are not well understood. In this paper, these effects are quantified for an idealized estuary using a one-dimensional, time-dependent numerical model. The numerical domain consists of a long, wide inlet and basin connected by a constricted channel. Kinetic power densities within this constriction are suitable for in-stream energy conversion. Modelling shows that the extraction of kinetic power has a number of effects, including: (a) reduction of the volume of water exchanged through the estuary over the tidal cycle; (b) reduction of the tidal range landward of the array; and (c) reduction of the kinetic power density in the tidal channel. These impacts are strongly dependent on the magnitude of kinetic power extraction, estuary geometry, tidal regime, and non-linear turbine dynamics. It is shown that it may be misleading to relate these impacts to the fraction of kinetic energy extracted from the system. Results highlight the importance of time-dependent modelling and the incorporation of non-linear turbine dynamics.

Keywords: tidal energy, numerical modelling

1 INTRODUCTION

The gravitational pull of the sun and moon on the earth's oceans produces a twice daily rise and fall in ocean depth. As the depth of the open ocean rises, water floods into estuaries and then, as the depth falls, ebbs back out. There has been a long-standing interest in harnessing this renewable resource to generate power because (a) areas with strong tides may be close to urban load centres and (b) tides are driven by gravitational forces rather than weather phenomena, making them predictable centuries in advance[**1**, **2**]. The semi-diurnal tidal cycle has a duration of 14.8 days. During this period, the strongest tides are referred to as spring tides and weakest as neap tides.

Within the past few years, new technology to extract kinetic power from tidal streams has reached an advanced demonstration phase. This approach uses free stream turbines to extract kinetic power from moving water and, unlike a barrage, does not require environmentally damaging impoundment behind a dam. Free-stream turbines superficially resemble the utility-scale wind turbines that have become a common feature of the energy landscape [**1**, **3**]. While methodologies exist for estimating the kinetic resource of tidal currents [**1**, **2**, **4**], a critical unknown is the level of extraction that will not result in unacceptable environmental impact. This is not expected to be an issue for proposed pilot facilities involving only a few turbines, but in order for the large-scale development of tidal in-stream energy to proceed, it will be necessary to understand an estuary's fluidic response to large-scale kinetic power extraction. Oceanographers and marine biologists will then be able to interpret these physical effects in a broader environmental context of ecosystem

Corresponding author: Department of Mechanical Engineering, University of Washington, Box 352600, Seattle, WA 98195, USA. email: bpolagye@u.washington.edu

processes to determine an environmentally acceptable level of extraction. Bryden and Melville [**1**], Bryden and Couch [**5**, **6**], Couch *et al.* [**7**], and Bryden *et al.* [**8**] have previously modelled extraction from steady-state flows. Garrett and Cummins [**9**, **10**] and Sutherland *et al.* [**11**] have formulated both analytical and computational representations of tidal currents driven by phase lags between large bodies of water.

In this study, the effects of extracting kinetic power from estuaries are investigated using a simple numerical model. Additionally, the effects of turbine nonlinearities (e.g. rated speed and cut-in speed) are explored. Section 2 lays out the underlying methodology; section 3 briefly reviews steady-state flows; section 4 considers an estuary forced by a constant period and amplitude wave at its inlet; and section 5 examines the more realistic case of an estuary forced by a neap-spring cycle.

2 METHODOLOGY

This study uses explicit, one-dimensional numerical models to capture the basic physics of large-scale kinetic power extraction from estuaries. The modelling of flows without kinetic power extraction is discussed in section 2.2 and the extension to flows with power extraction in section 2.3.

2.1 Model geometry

The geometry adopted for this study is a series of channels, each with constant cross-section. As shown in Fig.1, the model consists of a long, wide inlet connected to a long, wide basin by a short, narrow constriction. Depth differences between the inlet and the basin drive the flow through the constricted channel, where currents are fast enough to support extraction of kinetic power. This type of constricted channel is found in a number of locations; for example Admiralty Inlet and Tacoma Narrows in the Puget Sound.

2.2 Flow without kinetic power extraction

2.2.1 *Governing equations*

For one-dimensional, time-dependent flows, the fluid physics are described by the shallow water equations [**12**]. The formulations given below are specifically valid for situations: where (a) the entire

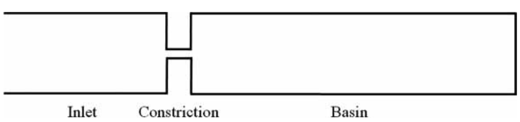

Fig. 1 Model geometry (top view)

water column moves with the particle velocity of the wave; (b) the pressure distribution is hydrostatic; (c) transient friction losses are treated using steady-state formulations; (d) the channel cross-section is rectangular and constant; (e) the channel bottom has no natural slope; and (f) Coriolis forces are neglected. The governing equations for mass and momentum may be written in conservation form as

$$\frac{\partial \overline{G}}{\partial t} + \frac{\partial \overline{F}}{\partial x} = -\overline{S} \tag{1}$$

where

$$\overline{G} = \begin{pmatrix} h \\ Q \end{pmatrix} = \begin{pmatrix} h \\ Uhb \end{pmatrix} \tag{2}$$

$$\overline{F} = \begin{pmatrix} Q/b \\ (Q^2/bh) + \frac{1}{2}gbh^2 \end{pmatrix} = \begin{pmatrix} hU \\ bhU^2 + \frac{1}{2}gbh^2 \end{pmatrix} \tag{3}$$

$$\overline{S} = \begin{pmatrix} 0 \\ ghbS_{\mathrm{f}} \end{pmatrix} \tag{4}$$

S_{f}, the friction slope, is given by the Manning formula [**13**]

$$S_{\mathrm{f}} = U|U|\frac{n^2}{R_h^{4/3}} \tag{5}$$

2.2.2 *Numerical solution to governing equations*

An explicit finite-difference approximation using the predictor-corrector MacCormack algorithm (second order in time and space) [**12**] is used to approximate the governing equations as

$$\overline{G}_j^{(1)} = \overline{G}_j^n - \frac{\Delta t}{\Delta x}\Big[(1-\varepsilon)\overline{F}_{j+1}^n - (1-2\varepsilon)\overline{F}_j^n - \varepsilon\overline{F}_{j-1}^n\Big] - \Delta t\overline{S}_j^n \tag{6}$$

$$\overline{G}_j^{(2)} = \overline{G}_j^n - \frac{\Delta t}{\Delta x}\Big[\varepsilon\overline{F}_{j+1}^{(1)} + (1-2\varepsilon)\overline{F}_j^{(1)} - (\varepsilon-1)\overline{F}_{j-1}^{(1)}\Big] - \Delta t\overline{S}_j^{(1)} \tag{7}$$

$$\overline{G}_j^{n+1} = \frac{1}{2}\left(\overline{G}_j^{(1)} + \overline{G}_j^{(2)}\right) \tag{8}$$

where ε is a parameter controlling the direction of differencing and its value is alternated between 0 and 1 on alternate time steps. For the inlet and basin $\Delta x = 100$ m and within the constriction $\Delta x = 50$ m. The grid is unstaggered. The value of Δt defaults to 2 s and is decreased as required to maintain the algorithm stability. At each time step, the Courant stability condition

$$\frac{|U| + \sqrt{gh}}{\Delta x / \Delta t} \leqslant 1 \tag{9}$$

is verified at each grid point and the time step size decreased and the step re-run, if the condition is exceeded.

Two types of boundary conditions are encountered: (a) internal at the junction of channels with different cross-sections and (b) external at either end of the numerical domain. While an initial condition must also be specified, if the first few tidal cycles are discarded, the selection of an initial condition is relatively unimportant and the case of high tide and zero velocity at all grid points yields stable performance during spin-up.

At internal junctions, downstream depth and velocity and upstream depth and velocity (four unknowns) are determined by solving the system of algebraic equations specified by the negative characteristic at the upstream boundary, positive characteristic at the downstream boundary, conservation of mass, and conservation of energy [**14**]. The four governing equations are solved simultaneously using Newton–Rhapson method with relaxation to guarantee convergence. A thorough discussion of the method of characteristics may be found in reference [**15**].

At the closed end of the basin, the boundary condition is specified as zero normal velocity, and the depth determined by the positive characteristic equation. The open boundary at the inlet must satisfy three criteria: (a) radiate internally generated waves without reflection; (b) allow external information to propagate into the system; and (c) maintain the mean sea level within the model domain when a periodic forcing is applied. Specifying the inlet depth, while a common approach, results in a clamped boundary that will reflect internally generated waves [**16**, **17**]. A more suitable formulation is proposed by Blayo and Debreu [**16**], which makes use of the Flather condition for the incoming characteristic (equation (10)) and extrapolation for the outgoing characteristic (equation (11)). Implicit in the formulation is the assumption that the shallow water phase speed is constant across the numerical boundary

$$U_0^{n+1} + \sqrt{\frac{g}{h_0^{n+1}}}\zeta_0^{n+1} = U_{\text{ext}}^{n+1} + \sqrt{\frac{g}{h_0^{n+1}}}\zeta_{\text{ext}}^{n+1} \tag{10}$$

$$U_0^{n+1} + \sqrt{\frac{g}{h_0^{n+1}}}\zeta_0^{n+1} = 2\left(U_1^{n+1} - \sqrt{\frac{g}{h_1^{n+1}}}\zeta_1^{n+1}\right) - \left(U_2^{n+1} - \sqrt{\frac{g}{h_2^{n+1}}}\zeta_2^{n+1}\right) \tag{11}$$

In the above formulations, the subscript ext refers to flow conditions external to the numerical domain and subscripts 0, 1, and 2 are respectively the first, second, and third model grid points from the open boundary. These two equations are solved simultaneously to give explicit formulations for velocity and depth on the numerical boundary. The external elevation (ζ_{ext}) is specified and external velocity (U_{ext}) is assumed to be zero.

2.3 Kinetic power extraction by in-stream turbines

Within the constricted channel, evenly spaced transects of in-stream turbines are positioned perpendicular to the flow. A schematic of a channel with four transects is shown in Fig. 2. It is assumed that the diameter of each turbine is very small in comparison to the channel geometry, which allows for a high blockage ratio. Three-dimensional flow features, such as the wake of each turbine, are of a length scale much smaller than is resolved on the numerical grid and kinetic power extraction can be approximated as occurring uniformly across a plane perpendicular to the flow. As such, extraction appears as a flow discontinuity and is modelled using a compatibility condition (analogous to the previous discussion for internal boundaries). This is similar to shock fitting, with the additional simplification that the location of the discontinuity is known *a priori*.

The energy compatibility relation (see Appendix 3 for derivation) across the extraction plane is given by

$$\frac{U_1^2}{2g}(1 - k_1) + h_1 = \frac{U_2^2}{2g}(1 - k_2) + h_2 \tag{12}$$

where station '1' is just upstream of the extraction plane and station '2' just downstream as shown in Fig. 2 and the extraction coefficient (k) for a transect is given by

$$k = \eta \frac{A_{\text{t}}}{A_{\text{c}}} \tag{13}$$

where A_{t} is the cross-section swept by the transect, A_{c} is the channel cross-section, and η is the coefficient of

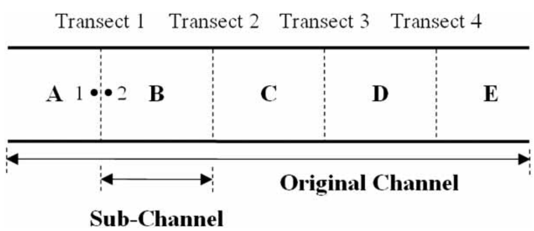

Fig. 2 Top view of channel with kinetic power extraction (channel segments labelled alphabetically). Dashed lines indicate transects. Numbered dots indicate 'upstream' and 'downstream' positions

performance. On flood tides, $k_1 = k$ and $k_2 = 0$, and vice versa on ebb.

Implicit in the above formulation is the assumption that transects will extract power from the flow in direct proportion to the free stream power for all velocities; that is, their behaviour is linear. In practice, turbines extract kinetic power in proportion to the free stream power only under a restricted set of conditions. Below the cut-in speed, the flow will be unable to overcome mechanical friction and the turbine will not rotate. Cut-in could be delayed beyond this point by pitch control or a mechanical brake. These dynamics are only valid for idealized systems in which the drag does not continue to increase above rated speed and the turbine support structure contributes negligibly to total drag. In design studies, the rated speed is chosen to achieve the lowest cost of energy [**18**]. As such, both parameters may be considered free variables for the purposes of investigation. A key question is whether these non-linearities play a meaningful role in the estuary response to extraction. That is, whether there are fluidic, as well as economic, implications to their selection.

The extraction coefficients in the energy compatibility relation may be modified to account for these non-linearities (see Appendix 3 for derivation)

$$\begin{aligned} k &= 0 && U < U_{\text{cut-in}} \\ k &= \frac{A_t}{A_c}\eta && U_{\text{cut-in}} \leqslant U \leqslant U_{\text{rated}} \\ k &= \left(\frac{U_{\text{rated}}}{U}\right)^3 \frac{A_t}{A_c}\eta && U > U_{\text{rated}} \end{aligned} \tag{14}$$

For both linear and non-linear transects, the blockage ratio (A_t/A_c) is assumed to be 50 per cent and the coefficient of performance (η) is 50 per cent. The classical Betz limit for a free-stream turbine is not used here since the downstream depth, and therefore pressure, will not be the same as the upstream depth, which represents a substantial departure from classical streamtube theory. A recent analytical investigation of theoretical extraction limits by Garrett and Cummins [**10**] concludes that the maximum extraction by an array of turbines evenly distributed across a channel is 33 per cent of the incident kinetic power. Therefore, the case considered here (25 per cent) is not the ideal upper limit, but simply a strenuous test case.

2.4 Forcings applied

Three types of forcing are applied to the water depth at the open boundary: (a) steady state; (b) constant amplitude and period sinusoid; and (c) a neap-spring cycle modelled with four constituent sinusoids.

2.4.1 *Steady state*

Steady-state flows have been investigated in up to three dimensions by Bryden *et al.* [**1**, **5**]. Steady flow is not the focus of this work, but a brief review helps to provide context for time-dependent modelling. For the steady-state model, the forcing is a constant driving head (depth difference) between the inlet and outlet of a channel. This is a simplified case of the geometry presented in Fig. 1.

2.4.2 *Constant amplitude and period sinusoidal forcing*

The simplest unsteady case is a forcing of constant amplitude and period. The external forcing at the system inlet is given by

$$\zeta_{\text{ext}}(t) = A \sin\left(2\pi \frac{t}{T}\right) \tag{15}$$

where ζ_{ext} is the elevation relative to mean sea-level external to the model. A period of 12.42 h models the principal semi-diurnal lunar tidal constituent (M2). This forcing allows an investigation of power extraction without the complications present when the system is being forced by multiple waves of varying amplitudes and periods, as in a neap-spring cycle.

2.4.3 *Neap-spring cycle*

Four constituent forcings are used to approximate the 14.8-day neap-spring tidal cycle. For this case, the elevation at the inlet boundary is specified by

$$\zeta_{\text{ext}}(t) = \sum_{i=1}^{4} A_i \sin\left(2\pi \frac{t}{T_i} - \theta_i\right) \tag{16}$$

where A_i, T_i, and θ_i are the amplitude, period, and phase lag of the ith constituent. The periods and amplitudes for the constituents are given in Table 1. For simplicity, it is assumed that all constituent phase lags are equal to zero. The type of tidal regime can be broadly characterized by the ratio of the strength of the diurnal (approximately 24 h period) and semi-diurnal

Table 1 Representative tidal constituents

		Amplitude		
Constituent	Period (h)	Semi-diurnal	Mixed (mainly semi-diurnal)	Mixed (mainly diurnal)
M2: principal lunar	12.421	1.3	1.2	0.83
S2: principal solar	12.000	0.48	0.4	0.32
K1: lunisolar declinational	23.934	0.1	0.9	1.68
O1: lunar declinational	25.819	0.1	1.5	0.98

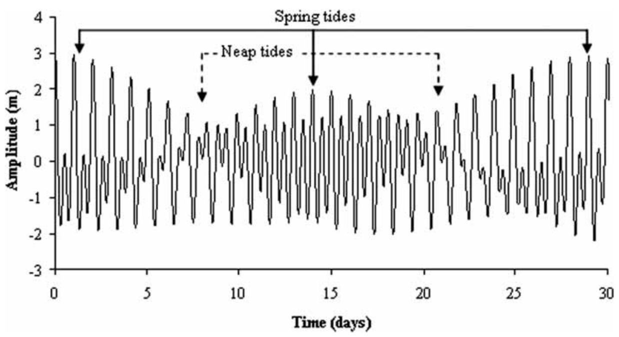

Fig. 3 Mixed, mainly semi-diurnal tide

constituents (approximately 12 h period) using the Formzahl (F) [**19**]. Three regimes described by their respective Formzahl are considered here:

1. F = 0–0.25: semi-diurnal tide with two high and low waters each day of approximately the same height.
2. F = 0.25–1.5: mixed, mainly semi-diurnal tide with two high and low waters each day, but with significant inequality in height and timing as shown in Fig. 3.
3. F = 1.5–3.0: mixed, mainly diurnal tide with either one high and low water each day, or two high and low waters with significant inequality in height and timing.

2.5 Method limitations

The modelling approach used has a number of limitations:

1. Channel velocity is assumed to be one-dimensional. Cross-channel and vertical variations in velocity cannot be resolved, nor are any local flow effects related to the turbine wake.
2. Channels are assumed to have constant, rectangular cross-sections.
3. Inlet forcing is assumed to be invariant with kinetic power extraction.

These limitations will be the most appropriately addressed by future work using more advanced models.

3 STEADY STATE

3.1 Approach

The steady-state approach uses a simplified geometry consisting of a single channel with a constant driving head. This means the depth of water is maintained at the inlet and outlet of the channel. While this constitutes a clamped boundary condition, and would produce spurious reflection in a time-dependent model, this is not a concern for modelling

Table 2 Steady-state base case geometry and forcing

Length (L)	3 km
Width (b)	1 km
Quiescent depth (D)	40 m
Manning roughness (n)	0.035
Driving head (H)	0.5 m

steady-state flow. Base case geometry and forcing are summarized in Table 2. Starting from a quiescent state, the driving head is imposed and the model spun-up to a steady-state over a half-day. The following quantities are then computed:

(a) flowrate (m^3/s) at the channel inlet;
(b) kinetic power (MW) at the channel inlet;
(c) kinetic power density (kW/m^2) at the channel inlet;
(d) kinetic power extracted (MW) by all transects.

The model is run for nine extraction cases – from no extraction up to eight transects.

3.2 Effect of kinetic power extraction

The impact of kinetic power extraction on the flow regime at steady-state is well-described by Bryden and Couch [**5**] and only a summary is given here. In order for the flow to satisfy both conservation of mass and energy, the water depth decreases and velocity increases across the plane of power extraction. As shown in Fig. 4(a), as the number of transects (N) increases, more of the driving head is consumed by power extraction and less is available to drive the flow. This is apparent in Fig. 4(b), which shows that the flow velocity is inversely related to power extraction. The local increase in velocity across each transect (not visible in Fig. 4(b)) is entirely subordinate to the channel-scale velocity decrease. Since the velocity increase across each transect is so minimal, power density is roughly constant along the channel and each transect extracts nearly the same amount of kinetic power from the flow.

The flowrate at the channel inlet as a function of the kinetic power extracted is shown in Fig. 5. While

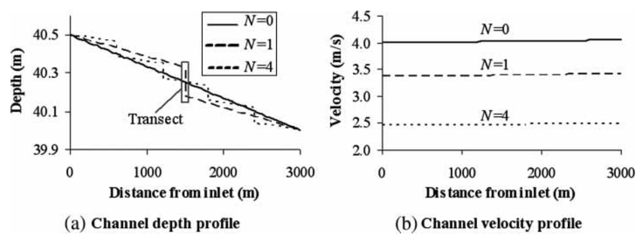

Fig. 4 Velocity and depth profiles for flows with 0, 1, and 4 transects (steady state, base geometry, and forcing)

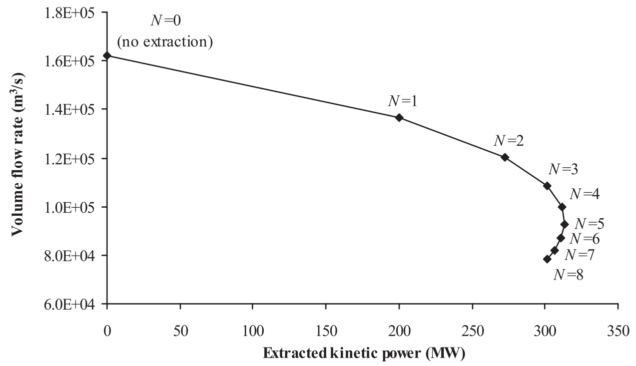

Fig. 5 Extraction impact (base steady-state forcing, base geometry)

each point represents a discrete number of linear transects, the curve is a continuous function of $\eta(A_t/A_c)N$ for a particular channel geometry and forcing. As a result, the choice of coefficient of performance (η) and blockage ratio (A_t/A_c) does not fundamentally alter the system response. For example, choosing a lower blockage ratio or coefficient of performance has the effect of moving all the points further down the same curve.

Extraction of kinetic power shows diminishing marginal returns since each additional transect reduces the velocity, and therefore, the kinetic power present in the system. Beyond a certain point, adding more turbines results in less power being extracted. This point of maximum power has been previously identified by Bryden and Couch [**6**] and Garrett and Cummins [**9**].

3.3 Dependence on geometry and boundary conditions

As shown in Fig. 6, the response to the extraction of kinetic power depends on channel geometry and boundary conditions (driving head). The solid black diamonds labelled 'Base Case' are identical to the curve shown in Fig. 5. These results are presented to contrast with the system response to time-dependent forcing, which is discussed in sections 4 and 5.

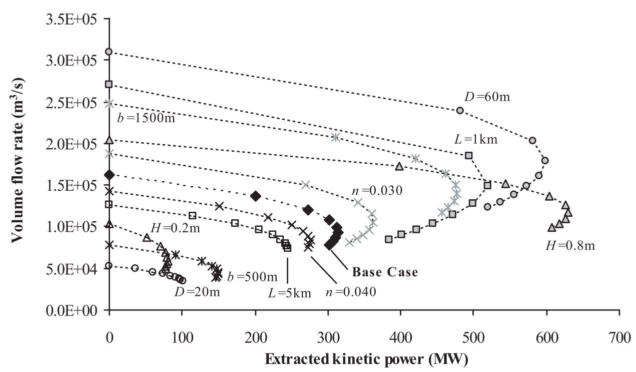

Fig. 6 Influence of geometry and driving head on extraction impact (base steady-state forcing). Curves are labelled by the perturbation about the base case: $L = 3\,\text{km}$, $b = 1\,\text{km}$, $D = 40\,\text{m}$, $n = 0.035$, and $H = 0.5\,\text{m}$

4 CONSTANT AMPLITUDE AND PERIOD SINUSOIDAL FORCING

4.1 Approach

The depth at the estuary inlet is sinusoidally forced by a wave of constant amplitude and period. Estuary geometry and forcing parameters are summarized in Table 3. Calculations are carried out for 3 days, which is sufficient to spin-up the model and eliminate the dependency on initial conditions. A number of quantities are monitored during ebb and flood tides at eight locations (black dots in Fig. 7) and a time-weighted average between the ebb and flood quantities is used to evaluate them over the complete tidal period. As in the steady-state case, energy extraction with up to eight transects is considered. Transects are located in the constriction between points 4 and 5 in Fig. 7. The monitored quantities are:

(a) flow volume exchanged across each plane (m^3);
(b) strength and time of peak velocity (ebb and flood) (m/s);
(c) depth and time of high and low tide (m);
(d) advected kinetic energy (MW) given by

$$\text{advected kinetic energy} = \left(\rho \frac{U^2}{2}\right) Uhb; \qquad (17)$$

(e) advected potential energy (MW) given by

$$\text{advected kinetic energy} = Uhb[\rho g(h+z)]; \qquad (18)$$

Table 3 Constant amplitude and period base case geometry and forcing

Inlet	
Length (inlet)	20 km
Width (b)	10 km
Basin	
Length (basin)	40 km
Width (b)	10 km
Constriction	
Length (L)	3 km
Width (b)	1 km
Entire system (estuary)	
Nominal depth (D)	40 m
Manning roughness (n)	0.035
Forcing amplitude (A)	3.0 m
Forcing period (T)	12.42 h

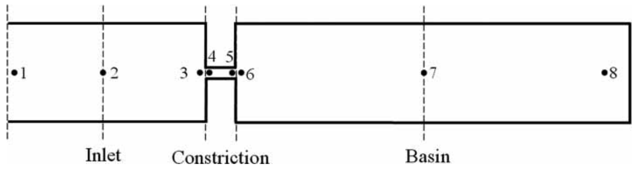

Fig. 7 Monitoring stations (top view)

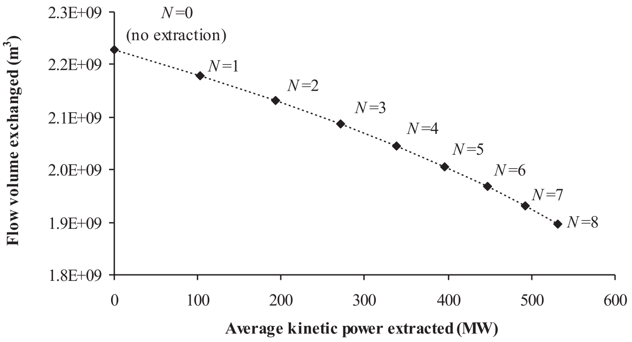

Fig. 8 Extraction impact (base constant amplitude and period forcing, base geometry)

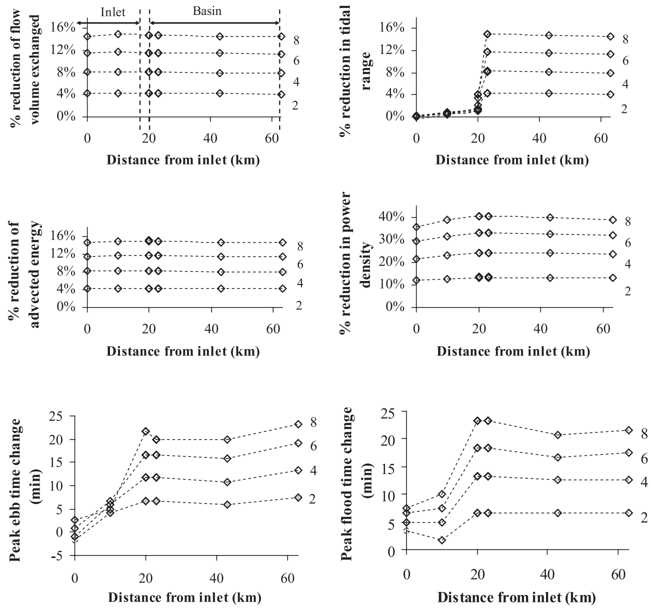

Fig. 9 Spatial variation in impacts of kinetic power extraction (base constant amplitude and period forcing, base geometry). Number of linear transects given to the right of each series

(f) kinetic power density (kW/m^2);
(g) kinetic energy extracted (MJ) and average kinetic power extracted (MW).

The tidal range is computed as the depth difference between high and low tides and the total advected energy as the sum of the potential and kinetic components.

4.2 Effect of kinetic power extraction

When kinetic power is extracted from a time-dependent system, the instantaneous flow structure within the constriction is similar to the steady-state case: velocity slightly increases across a turbine transect in the direction of the flow, and depth decreases. For the base case, the relation between cycle-average kinetic power extracted and reduction in flow volume exchanged across the constriction inlet is shown in Fig. 8. Increasing levels of extraction decrease the flow volume exchanged. As in the steady-state case, there is a decreasing marginal extraction for each additional transect.

Several cycle-averaged estuary-scale effects are also observed in proportion to the magnitude of extraction. The flow volume exchanged, tidal range, advected energy, and power density are reduced and the timing of tidal events is altered as shown in Figs 9(a) to (f). All flow quantities have been averaged over an ebb-flood cycle and normalized against their values without extraction. For both flow volume exchanged and advected energy reduction, there is little spatial variation within the estuary system and both have nearly the same value (Figs 9(a) and (c)). Range reduction shows substantially more spatial dependence, with almost no reduction at the inlet and significant reductions in the constriction and basin (Fig. 9(b)). The reduction in kinetic power density is the strongest impact noted, though it shows weak spatial variation (Fig. 9(d)). The change in timing varies for each tidal event (high tide, low tide, peak flood, peak ebb) and shows non-linear behaviour (e.g. timing change at constriction inlet in Fig. 9(e)). Of the effects considered, it is not apparent by inspection, which ones might cause the greatest environmental impact, though all are likely to have ecological implications. For example, reduced exchange volume would limit an estuary's ability to flush pollutants and a reduction in tidal range would be detrimental to mudflat ecosystems. Qualification of ecosystem impacts is beyond the scope of this paper and more appropriately addressed by oceanographers and biologists.

4.3 Comparison to steady-state results

For time-dependent systems, the point at which additional transects result in less total energy being extracted requires many more transects than in the steady-state cases discussed in section 3. In fact, none of the test cases considered in section 4.4 reach the point of maximum possible extraction. The underlying cause for this is a restorative feedback of the

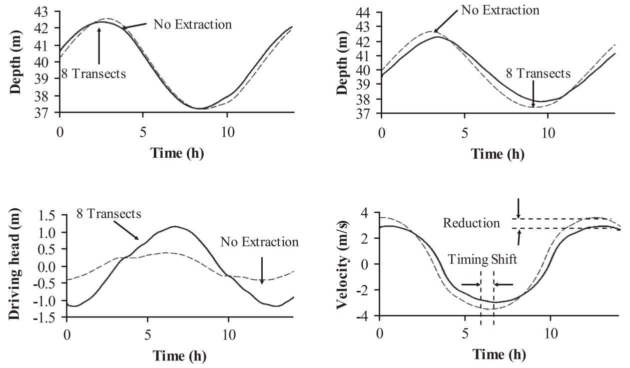

Fig. 10 Restorative forcing (base constant amplitude and period forcing, base geometry)

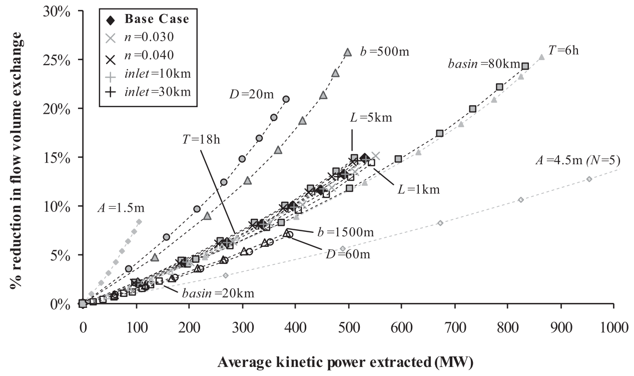

Fig. 11 Influence of geometry and boundary conditions on extraction impact (constant amplitude and period forcing). Curves are labelled by the perturbation about the base case

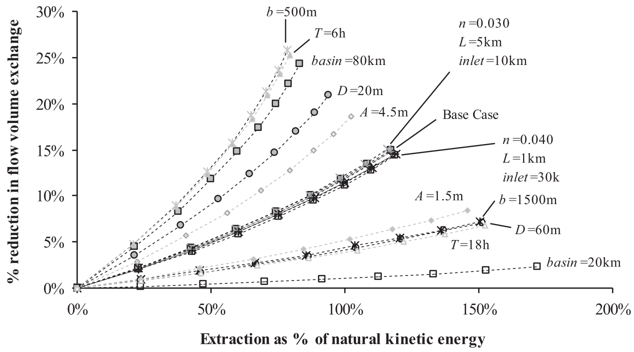

Fig. 12 Influence of geometry and boundary conditions on relative extraction impact (constant amplitude and period forcing). Curves are labelled by the perturbation about the base case

driving head in time-dependent systems. A constant driving head, such as in the steady-state case, will support a particular volume flowrate in a channel with a certain frictional resistance. As previously shown in Fig. 4, kinetic power extraction reduces the flowrate that can be supported by a constant driving head. In time-dependent cases with extraction, the depth does not change greatly at the constriction inlet (Fig. 10(a)), but because the basin is not being filled as quickly, the depth is lower at the outlet (Fig. 10(b)) in comparison to cases without extraction. Therefore, the driving head has increased (Fig. 10(c)). This partially offsets the velocity reduction that would be experienced in a system with a constant driving head, resulting in a smaller reduction and shift in the timing of peak velocity (Fig. 10(d)). In cases where tidal currents are driven by a phase lag at opposing ends of a channel [**9**], the restorative effect described here may be less important.

4.4 Dependence on geometry and boundary conditions

The influence of estuary geometry and boundary conditions (amplitude and period of forcing) on extraction impact, quantified as the reduction in flow volume exchanged, is shown Fig. 11. The absolute flow volume exchanged varies substantially between cases. In order to ease the comparison of impacts between different cases, flow volume reductions have been normalized as a percentage of their values without extraction. Of the geometric parameters tested, basin length, constriction ratio (ratio between width of basin and constriction), and constriction depth show the greatest influence. Constriction length, Manning roughness, and inlet length have relatively little impact on the system response. The amplitude and period of the external forcing have comparable influence on the system response compared with variations in geometry. These results suggest that in order to characterize the effect of kinetic power extraction from a constriction, the flow in the entire estuary, not just the constriction of interest, may have to be modelled.

At this point, it is useful to consider various methods of presenting impact data and the conclusions that can be drawn from these. From an economic perspective, it is desirable to extract the greatest kinetic energy with the fewest turbines. In Fig. 11, this corresponds to cases such as large basins or high amplitude forcing where the marginal increase in extracted power is highest for each additional transect. For engineering feasibility studies, in the absence of a fuller understanding of the effects of extraction, it has been common to limit extraction by in-stream turbines to a fixed percentage of the average kinetic resource without extraction (e.g. 15 per cent) [**18**]. This is arbitrary and not, in general, a useful metric. Figure 12 shows results for the same cases as Fig. 11, but for both a relative presentation of extraction and impact. Relative extraction is taken as the energy extracted by all transects divided by the kinetic energy entering the constriction over an ebb-flood cycle. The first implication of this figure is that relative impact does not correlate with the relative level of kinetic energy extraction between different cases. That is, for a particular fractional extraction (e.g. 75 per cent), the relative impacts vary considerably with geometry and forcing. This disconnect between impact and the fraction of the kinetic resource extracted is a logical corollary to Garrett and Cummins' analytical work, which shows that the point of maximum extraction for a tidal channel is uncorrelated with the kinetic resource in the undisturbed channel [**9**]. However, it is worth noting that extraction and impact are not entirely disparate since none of the cases tested produce a high reduction in flow volume exchanged for a low fractional extraction (e.g. 5 per cent). This indicates that pilot installations extracting a low fraction of the natural kinetic energy would be unlikely to significantly perturb the estuary-scale flow regime. Secondly, Fig. 12 is misleading since cases corresponding to a high level of relative extraction and low relative impact (e.g. geometric perturbation with a basin length of 20 km) appear desirable in relative terms, but extract too little power to be practical. In the near term, feasibility studies for commercial arrays will likely continue to assume an extraction level, which is a fixed percentage of the kinetic energy from the natural system. However, it is important to recognize that this does not generally guarantee that operation of such a tidal array would have an insignificant impact on the estuary-scale flow regime. As a result, it would be prudent for detailed case-by-case numerical model investigations be carried out for early stage commercial arrays.

In a number of cases shown in Fig. 12, the relative energy extracted is equivalent to more than 100 per cent of the kinetic energy in the natural tidal stream. This does not imply that the flow stops or reverses. Recall from section 3.2 that the kinetic power incident on each transect in a uniform channel is roughly constant and consider the hypothetical case of a channel with 100 MW of kinetic power at its inlet without extraction. If six transects each extract 20 MW of kinetic power from the flow, the total extracted kinetic power will be 120 MW, or 120 per cent of the kinetic power at the inlet without extraction. Further, the extraction of kinetic energy is primarily manifested as a decrease in potential energy, not as a decrease in kinetic energy and the kinetic energy in the system is only a small fraction of the total energy (potential and kinetic). This somewhat a counter-intuitive result follows from the realization that the kinetic and potential energies are not independently conserved in the flow. Rather their sum, less energy extracted by in-stream turbines, is conserved. Additional discussion may be found in Bryden and Couch [**6**].

4.5 Influence of transect non-linearity

The above discussions treat only linear transects and do not account for the non-linear dynamics of cut-in and rated speeds in real-world turbines. A representative comparison between the parameters for linear and non-linear transects is given in Table 4. As previously mentioned, the estuary response to extraction (e.g. Fig. 5) is a continuous function $\eta(A_t/A_c)N$ and changing the value of any of the parameters in the group shifts the response along the same curve. However, as shown in Fig. 13, the inclusion of cut-in and rated speeds fundamentally alters the system response – with the cut-in condition reducing impact and the rated condition increasing it. For both non-linearities, less kinetic energy is extracted from the flow for the same number of linear transects. This is to be expected, since both conditions result in a turbine giving up some of the energy in the flow, which would be extracted in the linear case. As the cut-in speed increases, additional low velocity flow passes through the transects unimpeded and the impact of extraction decreases. This is because low velocity flow accounts for a greater fraction of the flow volume exchanged than advected kinetic energy (since kinetic power depends on the cube of velocity while flow volume depends linearly). The increasing impact with lower rated speed can be similarly rationalized.

5 NEAP-SPRING CYCLE

5.1 Approach

The neap-spring cycle for a tidal regime is modelled by four constituent sinusoidal forcings of different amplitude and period. Base case geometry is the same as for the constant amplitude and period forcing (Table 3) and the base forcing is a mixed, mainly semi-diurnal tide (Table 1 and Fig. 3). This forcing is comparable to that seen in the Puget Sound. Transects are linear for the base case. Similar quantities to the constant amplitude and period case are monitored for each ebb and flood tide. Time-weighted averages are used to compare flow quantities over the 14.8-day neap-spring cycle.

Table 4 Linear and non-linear transect parameters

	Linear	Non-linear
η (%)	50	50
$A_t \cdot A_c^{-1}$ (%)	50	50
Cut-in speed (m/s)	0	0.5–2
Rated speed (m/s)	∞	1.5–3

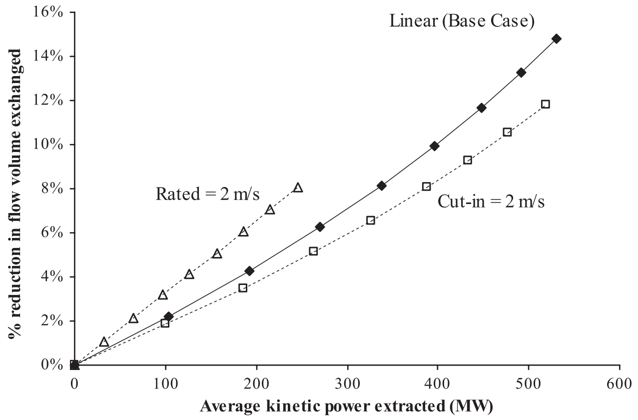

Fig. 13 Influence of non-linearity on extraction impact (base constant amplitude and period forcing, base geometry)

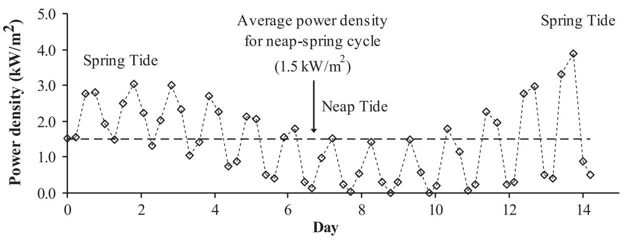

Fig. 14 Constriction power density (base neap-spring forcing, base geometry)

5.2 Effect of kinetic power extraction

For a mixed, mainly semi-diurnal tide, the amplitude and period of the tidal forcing change throughout the neap-spring cycle. As a result, the power density within the constricted channel also varies considerably from the neap-spring cycle average as shown in Fig. 14. Reductions in flow volume exchanged, range, and advected energy occur in relation to the magnitude of extraction but vary substantially over the cycle. Unlike the constant amplitude and period forcing, the value of the relative reduction in range is not always equal to the relative reductions in flow volume exchanged and energy advected, as shown in Fig. 15.

5.3 Dependence on geometry

Once flow quantities have been averaged over the neap-spring cycle, the relative influence of geometric parameters is essentially unchanged from the case of constant period and amplitude forcing. The relative reduction in flow volume exchanged for increasing levels of extraction is shown in Fig. 16. Again, constriction depth, constriction ratio (width of constriction compared with basin), and basin length have the greatest influence on extraction and its impact. Note that, in general, extracted power and relative

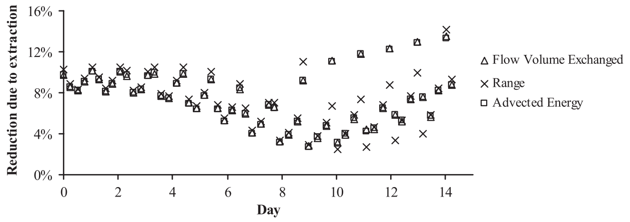

Fig. 15 Extraction impacts over neap-spring cycle (base neap-spring forcing, base geometry, eight transects). Each point represents the impact for an individual ebb or flood tide during the neap-spring cycle

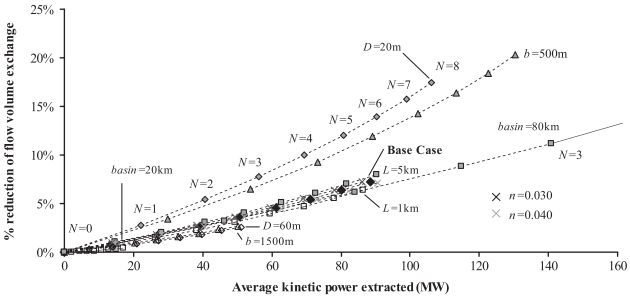

Fig. 16 Influence of geometry on reduction of flow volume exchanged (base neap-spring forcing). Curves are labelled by the perturbation about the base case. Results for the basin = 80 km perturbation are truncated

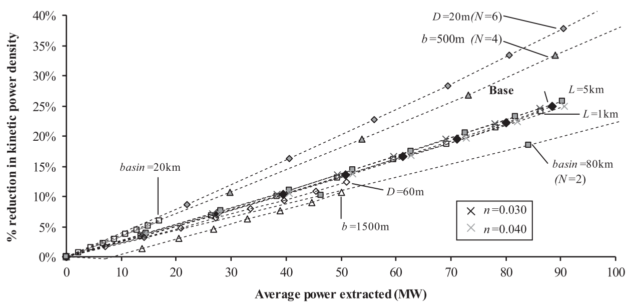

Fig. 17 Influence of geometry on reduction in kinetic power density (base neap-spring forcing). Curves are labelled by the perturbation about the base case. Results for the basin = 80 km, $D = 20$ m, and $b = 500$ m perturbations are truncated

impact are substantially lower than for the cases of constant amplitude and period forcing. This is because the constant amplitude and period forcing chosen corresponds to a continuous spring tide, which is unrealistically strong.

Figure 17 shows the relative reduction in kinetic power density in the constricted channel for the same cases as discussed above. This is an impact, which has not only environmental, but operational and design implications for in-stream arrays. Like other impacts, this reduction is dependent on estuary geometry and should not be neglected when estimating the power output in commercial-scale feasibility studies.

5.4 Dependence on tidal regime

For the neap-spring cycle, two types of forcing are tested: (a) varying the amplitude of all constituents by ±50 per cent for the mixed, mainly semi-diurnal regime and (b) forcing by semi-diurnal and mixed, mainly diurnal regimes (constituents given in Table 1). In order to make a meaningful comparison, all three regimes have been calibrated so that the cycle-averaged power density in the constriction does not vary between cases. The system response to extraction under different forcing regimes is shown in Fig. 18. For the same type of tidal regime (e.g. mixed, mainly semi-diurnal), higher amplitude forcing results in lower relative impact for the same absolute extraction. This result is anticipated from the constant period and amplitude modelling. Regime type also influences the system response to extraction, with greater semi-diurnal character resulting in greater impact for the test case considered here.

5.5 Influence of transect non-linearity

The influence of turbine non-linearity on reduction in flow volume exchanged is shown in Fig. 19 for the base case geometry and mixed, mainly semi-diurnal forcing. As in the case of constant amplitude and period forcing, lower rated speeds increase the extraction impact and higher cut-in speeds decrease the extraction impact. Again, both non-linearities substantially reduce the power extracted per transect. The relative effect of the rated and cut-in speed on the system response varies with the magnitude and type of tidal regime. For the mixed, mainly semi-diurnal tidal

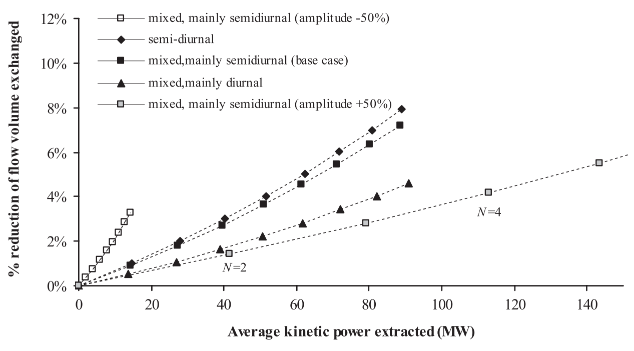

Fig. 18 Influence of tidal regime on extraction impact (base geometry). Curves are labelled by the perturbation about the base case. Results for the increased amplitude case are truncated

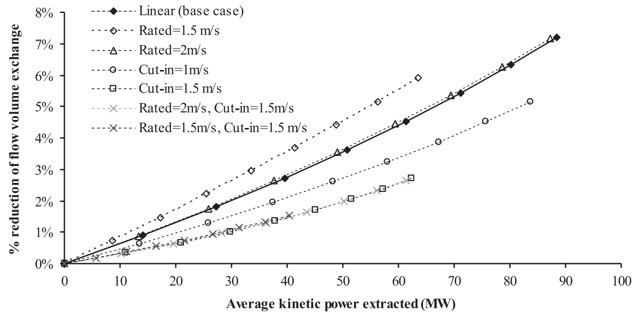

Fig. 19 Influence of non-linearity on extraction impact (base geometry, base neap-spring forcing). Curves are labelled by the perturbation about the base case

regime shown in Fig. 19, the system response to extraction is more strongly influenced by cut-in speed, as seen by the extreme and impractical example in which the rated and cut-in speeds are set equal. These results suggest that the selection of the rated and cut-in speed for an array of turbines can have significant fluidic implications, in addition to economic ones.

6 CONCLUSIONS

The extraction of kinetic power from estuaries has been shown to reduce flow volume exchanged, tidal range, advected energy, and kinetic power density, as well as alter the timing of the tides. The magnitude of these impacts is strongly dependent on the level of power extraction. For a particular estuary, the system response to extraction is determined by: (a) the estuary geometry; (b) tidal regime; and (c) non-linear turbine dynamics. All three must be accurately modelled to assess the impacts of in-stream tidal energy extraction on an estuary. While feasibility studies often set an extraction limit corresponding to a fraction of the natural kinetic power in an estuary system, the response to extraction does not correlate with the fractional level of extraction. This is a corollary to Garrett and Cummins' observations regarding the point of maximum possible extraction from a tidal channel [**9**]. Expressing extraction limits as a percentage of in-stream power is convenient, but has little underlying physical basis.

It has been shown that time-dependent analysis of kinetic power extraction from tidal streams is necessary to properly quantify the estuary-scale fluid impacts of extraction. Steady-state modelling, while instructive for some of the general physics, significantly overstates the impact of kinetic power extraction from tidal systems. Further, when considering non-linear transect dynamics, analysis over a full neap-spring cycle is necessary to assess the system response.

An encouraging result is that the effect of extraction is often relatively moderate, since even high levels of power extraction often correspond to reductions in the flow volume exchanged of less than 10 per cent. Because the response to extraction cannot be generalized at this time, appropriate extraction limits may have to be determined on a case-by-case basis. However, for initial pilot tests involving only a few turbines, the level of power extraction will be very low and large-scale fluidic impacts should be negligible. For the geometric and tidal variations tested, which are in-line with real estuaries, large-scale extraction for a neap-spring tidal cycle is on the scale of a small wind-farm (e.g. 100 + MW). This indicates that in-stream tidal energy has the potential to meaningfully contribute to regional energy demands.

Finally, if the marginal impact of each additional transect is low, extraction impacts may not be the limiting factor for array build-out. In real-world situations, the areas of high kinetic power density are often highly localized, which would require very tight turbine packing to accommodate a large number of transects. As inter-turbine spacing decreases, there exists the potential for the wake of an upstream turbine to degrade that of one downstream. Wake propagation, which is also not well understood for in-stream turbines, could limit array sizes more than estuary-scale environmental impacts. Further numerical and, particularly, experimental work in this area is required.

ACKNOWLEDGEMENTS

Brian Polagye would like to express his thanks to the Electric Power Research Institute and, in particular, Roger Bedard for providing fellowship funding for his doctoral research on tidal in-stream energy. He would also like to thank Dr James Riley, Dr Alberto Aliseda, and Dr Stephen Burges, all members of his PhD supervisory committee.

REFERENCES

1 **Bryden, I.** and **Melville, G.** Choosing and evaluating sites for tidal current development. *Proc. Instn Mech. Engrs, Part A: J. Power and Energy*, 2004, **218**(8), 567–577.
2 **Hagerman, G.** and **Polagye B.** Methodology for estimating tidal current energy resources and power production by tidal in-steam energy conversion (TISEC) devices. EPRI-TP-001 NA Rev 3, available from http://www.epri.com/oceanenergy, 2006.
3 **Bedard, R.** Survey and characterization: tidal in stream energy conversion (TISEC) devices. EPRI-TP-003 NA, available from http://www.epri.com/oceanenergy, 2005.
4 **Anon.** Phase II UK tidal stream energy resource assessment. Report to the Carbon Trust by Black and Veatch, available from http://www.carbontrust.co.uk, 2005.
5 **Bryden, I.** and **Couch, S.** ME1-marine energy extraction: tidal resource analysis. *Renew. Energy,* 2006, **31**(2), 133–139.
6 **Bryden, I.** and **Couch, S.** How much energy can be extracted from moving water with a free surface: a question of importance in the field of tidal current energy? *Renew. Energy,* 2007, **32**(11), 1961–1966.
7 **Couch, S., Sun, X.,** and **Bryden, I.** Modeling of energy extraction from tidal currents. In Proceedings of the 6th European Wave and Tidal Energy Conference, EWTEC 2005, Glasgow, August 2005, Glasgow, UK.
8 **Bryden, I., Couch, S., Owen, A.,** and **Melville, G.** Tidal current resource assessment. *Proc. IMechE, Part A: J. Power and Energy*, 2007, **221**(A2), 125–135.
9 **Garrett, C.** and **Cummins, P.** The power potential of tidal currents in channels. *Proc. R. Soc. A.*, 2005, **461**, 2563–2572.
10 **Garrett, C.** and **Cummins, P.** The efficiency of a turbine in a tidal channel. *J. Fluid Mech.*, 2007, **588**, 243–251.
11 **Sutherland, G., Foreman, M.,** and **Garrett, C.** Tidal current energy assessment for Johnstone Strait, Vancouver Island. *Proc. IMechE, Part A: J. Power and Energy*, 2007, **221**(A2), 147–157.
12 **Garcia-Navarro, P.** and **Saviron, J.** McCormack's method for the numerical simulation of one-dimensional discontinuous unsteady open channel flow. *J. Hydraulic Hydraul. Res.*, 1992, **30**(1), 95–105.
13 **Wilcox, D.** *Basic fluid mechanics*, 2nd edition, 2000 (DCW Industries, La Cañada, California).
14 **Chaudhry, M.** *Applied hydraulic transients*, 1979 (Van Nostrand Reinhold Company, New York).
15 **Liggett, J.** and **Cunge, J.** Numerical methods of solution of the unsteady flow equations. In *Unsteady flow in open channels* (Eds K. Mahmood and V. Yevjevich), vol. II, 1975 (Fort Collins, Colorado).
16 **Blayo, E.** and **Debreu, L.** Revisiting open boundary conditions from the point of view of characteristic variables. *Ocean Model.*, 2005, **9**(3), 231–252.
17 **Chapman, D.** Numerical treatment of cross-shelf open boundaries in a barotropic coastal ocean model. *J. Phys. Oceanogr.*, 1985, **15**, 1060–1075.
18 **Polagye, B.** and **Previsic, M.** System level design, performance, cost and economic assessment – Tacoma Narrows Washington tidal in-stream power plant. EPRI-TP-006 WA, available from http://www.epri.com/oceanenergy, 2006.
19 **Defant, A.** *Physical Oceanography*, vol. II, 1961 (Pergamon Press, New York).

APPENDIX 1

Notation

A	amplitude of forcing adjacent to open boundary (m)
A_c	channel cross-sectional area (m^2)
A_t	swept area of transect (m^2)
b	width of channel segment (m)
basin	length of estuary basin (between constricted channel and closed end) (km)

D	reference water depth (m)
g	acceleration due to gravity (9.81 m/s^2)
h	water depth (m)
h_j^n	water depth at grid point j and time n (m)
H	driving head (m)
inlet	length of estuary inlet (between ocean and constricted channel) (km)
k	loss coefficient or extraction coefficient (dimensionless)
L	length of constricted channel (m)
n	Manning roughness coefficient (s/m$^{1/3}$)
N	number of transects
Q	volume flowrate of water (m^3/s); $Q = Uhb$
R_h	hydraulic radius (m)
S_f	friction slope (dimensionless)
t	time from start of simulation (s)
T	period of forcing adjacent to open boundary (h)
U	water velocity (m/s)
U_j^n	velocity at grid point $j$and time n (m/s)
z	common reference elevation for computation of advected potential energy (m)
Δt	time step on numerical domain (s)
Δx	distance between grid points in numerical domain (m)
ζ	water surface elevation relative to reference depth (m)
η	coefficient of performance for transect (dimensionless)
θ	phase lag of harmonic constituent (radians)

APPENDIX 2

1. Blockage ratio: the swept area of all turbines on a transect divided by the cross-sectional area of the channel (A_t/A_c).
2. Capacity factor: ratio of average extracted kinetic power over measurement period to maximum extracted kinetic power during the same period.
3. Driving head: depth difference between inlet and outlet of constricted channel.
4. Extraction effectiveness: the ratio of cycle-average kinetic power extracted to reduction in a reference flow value (normally flow volume exchanged). The higher the effectiveness, the lower the environmental footprint of an array of in-stream turbines for a given level of extraction.
5. Extraction impact: the alteration of estuary-scale flow parameters in response to kinetic energy extraction. The higher the impact, the greater the reduction in a parameter from the natural baseline. Unless otherwise stated, impact is characterized by the reduction in flow volume exchanged.
6. Flow volume exchanged: the total volume of water passing through a plane perpendicular to the flow during an ebb or flood tide.
7. Kinetic power density: the kinetic power per cross-sectional unit of the flow and is given by $P = 0.5\rho U^3$ where ρ is the density of seawater (1024 kg/m^3) and U the magnitude of the free-stream velocity. All power densities discussed here are kinetic.
8. Natural: reference baseline for a flow quantity (e.g. power density) without extraction by in-stream turbines.
9. Tidal range: the difference in elevation between high and low tides.
10. Time-dependent: a model in which the flow quantities at a given point in space change with time, in contrast to steady-state flow in which the flow quantities are time-invariant at a given point in space.
11. Transect: a row of in-stream turbines perpendicular to the flow in a channel. Two types are considered: linear and non-linear as discussed in section 2.3.

APPENDIX 3

Energy compatibility condition for kinetic power extraction

In general, the total upstream potential and kinetic power must equal the total downstream potential and kinetic power plus the power extracted at the turbine transect

$$\mathrm{PE}_1 + \mathrm{KE}_1 = \mathrm{PE}_2 + \mathrm{KE}_2 + \text{extraction}$$

Case 1: linear transect

If we restrict ourselves to the case of a flood tide, then

$$\text{Extraction} = \frac{1}{2}\rho U_1^3 A_t \eta$$

and the balance between the flux of kinetic and potential energy may be written as

$$(\rho U_1 h_1 b) g h_1 + (\rho U_1 h_1 b)\frac{1}{2}U_1^2 = (\rho U_2 h_2 b) g h_2 + (\rho U_2 h_2 b)\frac{1}{2}U_2^2 + \frac{1}{2}\rho U_1^3 A_t \eta$$

Noting that due to mass conservation

$$\rho U_1 h_1 b = \rho U_2 h_2 b$$

and defining the channel area as

$$A_c \equiv h_1 b$$

then the conservation equation may be simplified to

$$\frac{U_1^2}{2g}\left(1-\eta\frac{A_t}{A_c}\right)+h_1=\frac{U_2^2}{2g}+h_2$$

Case 2: non-linear transect operating at or above rated speed

For the case of a non-linear turbine operating at or above rated speed, then if we again take the case of a flood tide, extraction may be written as

$$\text{Extraction}=\frac{1}{2}\rho U_{\text{rated}}^3 A_t \eta$$

the conservation equation may be written as

$$(\rho U_1 h_1 b) g h_1+(\rho U_1 h_1 b)\frac{1}{2}U_1^2=(\rho U_2 h_2 b) g h_2$$
$$+(\rho U_2 h_2 b)\frac{1}{2}U_2^2+\frac{1}{2}\rho U_{\text{rated}}^3 A_t \eta$$

and comparably simplified to

$$g h_1+\frac{1}{2}U_1^2=g h_2+\frac{1}{2}U_2^2+\frac{1}{2}\frac{U_{\text{rated}}^3}{U_1}\frac{A_t}{A_c}\eta$$

which may be expressed as

$$\frac{U_1^2}{2g}\left[1-\left(\frac{U_{\text{rated}}}{U_1}\right)^3\frac{A_t}{A_c}\eta\right]+h_1=\frac{U_2^2}{2g}+h_2$$